Use of beam parameters in optical component testing

D. R. Neal*, J. K. Gruetzner*, J.P. Roller*
WaveFront Sciences, Inc., 14810 Central S.E. Albuquerque, NM 87123

ABSTRACT

We are investigating the use of a Shack-Hartmann wavefront sensor for measuring optical component quality during manufacture and testing. In a variety of fields, an optical component is designed to pass an optical signal with minimal distortion. Quality control during the manufacturing and production process is a significant concern. Changes in beam parameters, such as RMS wavefront deviation, or the beam quality parameter M^2, have been considered as indications of optical component quality. These characteristics can often be quickly determined using relatively simple algorithms and system layouts. A laboratory system has been prepared to investigate the use of a wavefront sensor to measure the quality of an optical component. The instrument provides a simultaneous measure of changes in M^2 and induced RMS wavefront error. The results of the investigation are presented.

Keywords: optical testing, beam quality, M^2, wavefront error, Shack-Hartmann, Hartmann-Shack

1. INTRODUCTION

Optical systems and components have become ubiquitous in modern society. Advanced laser technologies, optics, and electronics are often combined into devices such as compact disk recorders and fiber optic networks, which were unknown a generation ago. With the explosive growth of photonics industries, optical components are being produced and mass-produced at a scale unprecedented in history.

Component producers and manufacturers have a critical interest in the quality of their products. Sample testing is typically not sufficient. Each item must be tested to ensure that it operates within specifications. As a result, each item is often passed through a number of tests. Desirable test qualities include precision, accuracy, cost, training requirements, and speed.

Many different measures are used to specify the quality of optical components. Optical measurements refer to the effect the component has on light transmitted through it or reflected from it. These include transmittance, reflectance, and aberrations. In a number of applications, the underlying desire is to determine how the component transforms a beam or pulse of light with respect to its propagation through the rest of the system. In theory, actually performing such propagation is the best testing method. Where this is impractical or otherwise undesirable, a suitable surrogate must be found that can be used to estimate component performance.

Especially for components used to control and direct laser beams, it seems natural to evaluate the effect of each component on the beam quality of the laser itself. Modern tools can be used to rapidly evaluate the beam quality, leading to a quick and accurate measure of the effect of a given optic on the performance of the optical system.

The problem is that the calculation of the beam parameters must be performed in an accurate manner. Since estimation of these parameters may involve a series of complex mathematical operations, there is the reality that any particular beam parameter may not be the best measure of component quality.

In some cases, especially where imaging is involved, it is possible or desirable to characterize the component in terms of the Seidel aberrations it induces. Aside from often being difficult and time consuming, this method is not appropriate in many other instances. Two measurements that may be more appropriate are the beam quality parameter M^2 and the root-mean-square wavefront error. It is possible to measure these parameters easily and quickly using a Shack-Hartmann wavefront sensor and associated software.

2. MEASURES OF QUALITY

2.1 Beam quality parameter M^2

In 1971, Marshall[1] introduced a simple way of quantifying beam quality, similar to the common usage of specifying the "number of times diffraction limit",[2] which provides a relationship between the near-field beam size and the far field beam spread. A beam quality parameter M^2 was introduced[3] to provide a quantitative measurement of the quality of mixed mode Gaussian-Laguerre (hereafter just Gaussian) beams, using the TEM_{00} mode as a reference. M^2 has become the most commonly used indicator of beam quality.

M^2 is based upon the space-beamwidth product for a given laser beam, analogous to the time-bandwidth product for the propagation of a Gaussian signal.

$$M^2 \equiv 4\pi\sigma_{0x}\sigma_{s_x}, \tag{1}$$

where the second moments are defined by,

$$\sigma_x^2(z) = \int_{-\infty}^{\infty}\int (x-\bar{x})^2 |E(x,y,z)|^2 dxdy, \text{ and} \tag{2}$$

$$\sigma_{s_x}^2 = \int_{-\infty}^{\infty}\int (s_x-\bar{s_x})^2 |\Im\{E(x,y,z)\}|^2 ds_x ds_y, \tag{3}$$

$\bar{x}$ is the location of the intensity centroid in x at the origin $z = 0$, $\bar{s_x}$ is the frequency space intensity centroid, $\Im\{\ \}$ is the Fourier transform from normal space (x, y) to frequency space (s_x, s_y), and E is the field amplitude of the laser beam. σ_{0x} is the value at $\sigma_x(z = 0)$. The convention is for a paraxial beam propagating along the z-axis. M_y^2 is obtained in a similar fashion. The subscript denoting x- or y-axis will generally be suppressed in the remainder of this paper.* It can be shown that σ_s is independent of z.

The practical value of M^2 lies in its ability to describe the spread of a beam's intensity as it propagates.

$$w^2(z) = w_0^2\left[1 + \left(\frac{M^2\lambda z}{\pi w_0^2}\right)^2\right] \tag{4}$$

where beam size $w(z) = 2\sigma(z)$, $w_0 \equiv w(z=0)$, and λ is the wavelength. If M^2 and the beam size at any point are known, the beam size at any location along the beam path can be calculated.

2.2 Change in absolute RMS wavefront deviation

Another traditional method for measuring the quality of an optical component is to measure the effect of the optic on the RMS or peak-to-valley optical wavefront. The RMS wavefront error is defined from the measured wavefront surface ϕ,

$$\phi_{RMS} = \sqrt{\frac{\iint(\phi(x,y)-\bar{\phi})^2 dxdy}{\iint dxdy}} \tag{5}$$

---

* Some authors define M^2 equivalently in terms of beam diameter, wavelength, and far-field divergence angle. M^2 has also been defined in terms of radii other than the second moment; the definition used here is the most common.

This test can be performed in either transmission or reflection. The drawback of this technique is that a means of measuring the wavefront (or phase) is needed in order to calculate the appropriate quantities. For a system based on the Shack-Hartmann wavefront sensor, these parameters are automatically calculated. In fact, the RMS wavefront error is calculated directly from the reconstructed wavefront. The beam parameters (M^2, etc.) are also calculated using the reconstructed wavefront. However, this calculation involves many more steps, which may introduce errors in the results.

3. MEASUREMENT WITH A SHACK-HARTMANN WAVEFRONT SENSOR

The Shack-Hartmann wavefront sensor is capable of measuring the full irradiance and phase distribution of a laser beam. Incident light is sampled, using a lenslet array image dissector, into a number of small regions (as shown in Figure (8)). The wavefront is assumed to be linear across each of these samples. For sufficiently small samples, this assumption is usually accurate. The wavefront slope of the light incident upon each of these samples is determined by computing the differences in locations of the focal spots on a detector array. A centroiding or other algorithm may be used to compute the position of the spots and, after comparison to a reference set of locations, the wavefront slope at each point may be obtained. This map of the wavefront slope is then integrated (using any of several methods) to provide the wavefront. The irradiance distribution is obtained from the total light in each focal spot.

The wavefront sensor has significantly lower spatial resolution than the CCD array itself. The higher spatial resolution of the CCD has essentially been traded for the ability to measure phase. In general, the phase changes relatively slowly across the aperture (for most optical systems), so a good measurement is obtained even when using a relatively small number of samples.

3.1 Calculation of RMS error from wavefront sensor data

The RMS wavefront error can be calculated directly from the reconstructed wavefront using equation(5), replacing the integrations with summations. In most cases, the tilt would first be removed from the measured wavefront in order to evaluate only the effects of focus and other higher order terms on the RMS error.

3.2 Calculation of M^2 from wavefront sensor data

Given that an accurate determination of the irradiance and phase can be made using the wavefront sensor, an estimate of M^2 and other beam parameters can also be obtained from application of the appropriate algorithm.

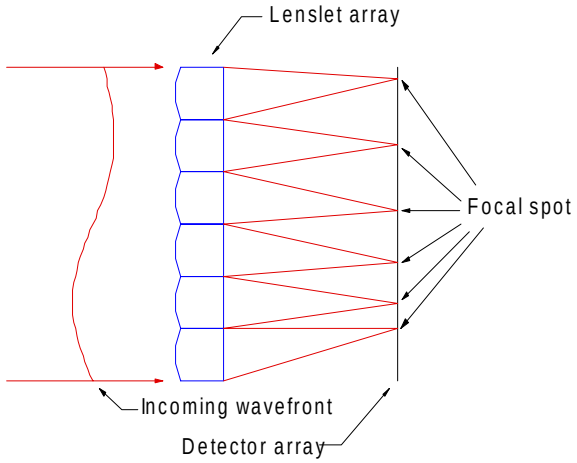

Figure 8: Basic layout of Shack-Hartmann wavefront sensor.

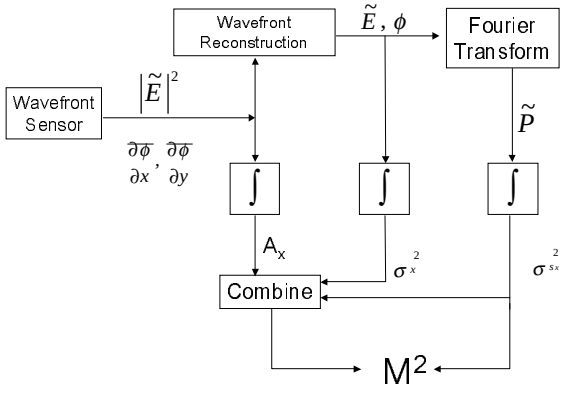

Figure 2: Algorithm for computing M^2 using the gradient method.

There is a significant advantage to calculating the beam parameters from a Shack-Hartmann wavefront sensor: the beam parameters can be determined from a single measurement. This allows rapid determination of many beam parameters. Furthermore, it allows characterization of pulsed lasers or beams that are fluctuating in time. While application of the ISO standard[4] allows for extremely accurate measurement of M^2 in some situations, it is very time-consuming and requires the application of careful measurement processes. It fails totally for a laser that is fluctuating during the measurement time.

There are many different methods for estimating the beam parameters from wavefront sensor data.[5] It has been observed that the accuracy of these estimates varies according to the method.[6] In the following sections, each of the different methods will be described and compared.

3.3 Gradient method

The gradient method of obtaining M^2 from a Shack-Hartmann wavefront sensor is based upon an analysis first developed by Siegman. It is based upon Fourier analysis of a laser beam. The complex electrical field distribution of a beam directed along the z-axis can be given by $\tilde{E}(x, y, z)$, with the corresponding description in the spatial frequency domain given by its Fourier transform, $\tilde{P}(s_x, s_y, z) = \Im\{\tilde{E}(x, y, z)\}$. Beam intensities in each domain are then defined by $I(x, y, z) \equiv \left|\tilde{E}(x, y, z\right|)^2$, and $I(s_x, s_y, z) \equiv \left|\tilde{P}s_x, s_y, z\right|^2$. Equations (1)–(4) are used to determine M^2 from the second order moments of the irradiance distribution.

For a paraxial beam in the z-direction, with an arbitrary reference plane (x, y, z_1), the intensity standard deviation will have the value

$$\sigma_x^2 = \sigma^2(z_1) - A_{x,1} \times (z - z_1) + \lambda\sigma_{s_x}^2 \times (z - z_1)^2 \tag{6}$$

where $A_{x,1}$ is given by the function

$$A_{x,1} \equiv A_x(z_1) = \frac{\lambda}{\pi P}\int_{-\infty}^{\infty}\int x\left|\tilde{E}(x, y, z)\right|^2 \frac{\partial\phi(x, y, z)}{\partial x} dxdy \tag{7}$$

where $\phi(x,y,z)$ is the phase. Note that the partial derivative of the phase with respect to x is the wavefront x-slope, which is one of the outputs from a Shack-Hartmann wavefront sensor.

The location of the beam waist can be found by minimizing equation (6),

$$(z_{x_0} - z) = \frac{A_{x,1}^2}{2\lambda^2\sigma_{s_x}^2}. \tag{8}$$

Substituting back into equation (6) yields the relationship,

$$\sigma_{x_0}^2 = \sigma^2(z_1) - \frac{A_{x,1}^2}{4\lambda^2\sigma_{s_x}^2} \tag{9}$$

M_x^2 follows immediately from equation (1).

This method is readily implemented computationally by replacing the integrals with sums over the areas of a Shack-Hartmann sensor. The sequence is as follows (see Figure (2)). From the Shack-Hartmann sensor, the distribution of intensity, $I(x, y, z_1)$, and wavefront slopes, $\frac{\partial\phi}{\partial x}$ and $\frac{\partial\phi}{\partial y}$, are obtained at a reference plane. After wavefront reconstruction, the electric field,

$$\tilde{E}(x, y, z_1) = E(x, y, z_1)exp(i\phi(z, y, z_1)) \tag{10}$$

is calculated, and the spatial-frequency electric field distribution is obtained by means of a Fourier transform algorithm, such as the Fast Fourier transform (FFT). The M^2 values can then be calculated following the procedure given above.

3.4 Curvature removal method

This method relies on a fit to the wavefront data to produce an artificial waist and on the Fourier transform of the field to find the far-field divergence. First, the irradiance and phase distributions are used to create the complex electric field

$$E(x, y) = \sqrt{I(x, y)}\, e^{j2\pi w(x, y)/\lambda} \tag{11}$$

This is then propagated to the far-field using the Fourier Transform method,

$$E'(u, v) = \iint E(x, y) e^{jk(xu + yv)} dxdy\,. \tag{12}$$

The far-field irradiance distribution is calculated using

$$I'(u, v) = |E'(u, v)|^2\,. \tag{13}$$

The second moment of this distribution is then computed within specified limits,

$$\sigma^2_{x,FF} = \frac{\int_{y_1}^{y_2}\int_{x_1}^{x_2} I'(u, v)(u - \bar{u})^2 du dv}{\int_{y_1}^{y_2}\int_{x_1}^{x_2} I'(u, v) du dv}\,, \tag{14}$$

where the limits of integration may be determined either by a threshold or as a specified multiple of the second moment itself in a self-convergent sense.* The far field divergence is then expressed (already in angular space) as

$$\Theta_x = 4\sigma_{x,FF}\,. \tag{15}$$

The wavefront curvature is computed using a least-squares fit to a circle,

$$S(x, y) = \frac{x^2}{R_x} + \frac{y^2}{R_y}\,. \tag{16}$$

The average wavefront curvature *S(x,y)* is subtracted from the input wave. This curvature removal creates a beam with infinite radius of curvature. By definition, this is now a waist, and the beam size can be calculated *at that position* using Equation (2). The curvature-removed far-field is calculated using Equation (12). The value of M^2 can now be determined as

$$M_x^2 = \frac{\pi}{\lambda}\sigma_x \Theta_{x,CR}\,, \tag{17}$$

where the curvature-removed wavefront was used to compute $\Theta_{x,CR}$ from the Fourier transform.†

The true far-field divergence angle is computed using a Fourier transform of the original field. Knowing the far-field divergence angle and M^2, the actual waist size is (not the "curvature removed" waist size) is calculated by

---

* More detail on the second moment definition and its applications may be found in reference (4).

† This is often written $M_x^2 = \frac{\pi}{4\lambda} d_x \Theta_{x,CR}$, where $d_x = 4\sigma_x$, following the notation of reference (4).

$$d_{0x} = \frac{4}{\pi}\frac{M_x^2}{\Theta_x}, \tag{18}$$

and the waist position is

$$(z - z_0)^2 = \frac{d_x^2 - d_{0x}^2}{\Theta_x^2}. \tag{19}$$

The beam width propagation equation is then straightforward,

$$d_x^2 = d_{0x}^2 + \Theta_x^2 (z - z_0)^2. \tag{20}$$

3.5 Multi-propagation method

The multiple propagation method relies on the fact that the complete irradiance and phase distribution provide sufficient information for a numerical evaluation of the beam at a downstream or upstream location. The field described in equation (11) can be propagated to a new location using the Fresnel integral:

$$E'(x', y') = \frac{e^{jkz}}{jkz}\int_{-\infty}^{\infty}\int E(x, y) Exp\left[j\frac{k}{2z}[(x - x')^2 + (y - y')^2]\right]dxdy. \tag{21}$$

This operation can also be performed using a Fast Fourier Transform (FFT).

The multiple-propagation M^2 method propagates the beam numerically to a number of different z-locations, calculates the 2nd moment spot size at each location, and fits the resulting beam widths to equation (11).

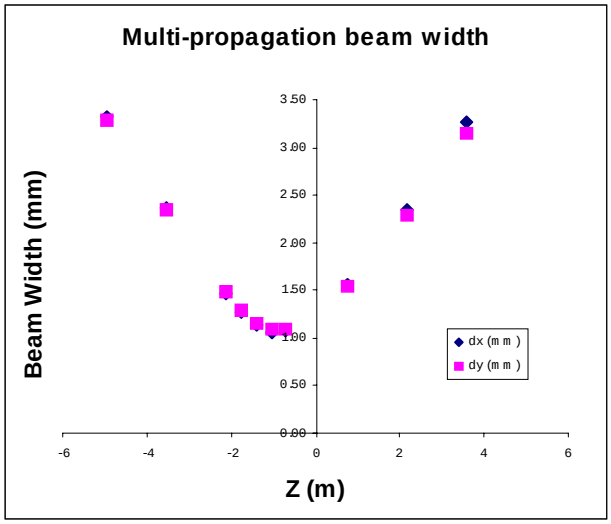

Figure 3: ISO standard beam widths as a function of beam position after multi-propagation analysis.

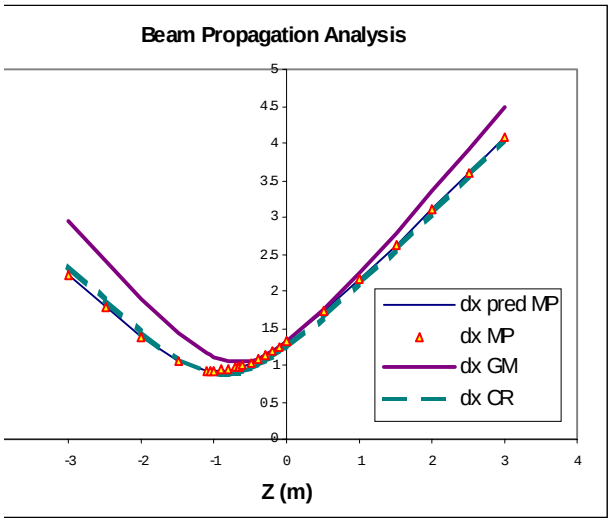

Figure 4: Comparison of Multi-Propagation (MP), Gradient (GM) and Curvature Removal (CR) methods. The MP method shows both the calculated beam widths (points) and the predicted values (curve).

The local beam divergence and spot size are also useful parameters. Together with M^2, they can be used to determine the Gaussian beam characteristics at a further plane. The local beam divergence is

$$\theta_x = 4\frac{\sigma_x}{R_x}. \tag{22}$$

The Rayleigh range can also be computed from the beam parameters. It is defined as:

$$Z_R = \frac{\pi}{4\lambda}\frac{d_{0x}^2}{M_x^2} \tag{23}$$

3.6 Moments method

The moments method relies on the fact that the cross moments of the irradiance distribution contain useful information. Specifically[8,9]:

$$d_x = 4\sqrt{\langle x^2\rangle}, \tag{24}$$

$$\theta_{\sigma x} = 4\sqrt{\langle u^2\rangle}, \tag{25}$$

$$M_x^2 = \frac{4\pi}{\lambda}\sqrt{\langle x^2\rangle\langle u^2\rangle - \langle xu\rangle^2}, \tag{26}$$

where

$$\langle u^2\rangle = -\frac{k}{P}\iint\left[\left(\frac{\dfrac{\partial I_m(\vec{x};z)}{\partial x}}{4I_m(\vec{x};z)}\right) - k^2 I_m(\vec{x};z)\cdot\left(\beta_m^x(\vec{x};z)\right)^2\right]dxdy. \tag{27}$$

he cross moment $\langle xu\rangle$ is also the radius of curvature of the beam at the measurement location. This method has been used recently by several authors in evaluating the accuracy of making M^2 measurements with Shack-Hartmann wavefront sensors.[5,8,9] In many ways, this method is similar to the gradient method.

3.7 Comparison of results

These different methods for calculating the beam parameters from the irradiance and phase distributions have vastly different responses to errors in the input field. They each have their strengths and weaknesses. The gradient method and the moments method can each be calculated very quickly. Both rely on no more than one Fourier transform, and both use the wavefront slope information that is produced directly by the wavefront sensor. At first glance, it would seem appropriate to use information that is closest to the direct measurement, with a minimum of additional algorithms. Certainly variations in the wavefront reconstructor are not an issue in the moments method, and they are even less so in the gradient method.

However, the moments and gradient methods each rely (implicitly or explicitly) on the spatial derivatives of the entire E-field. This includes spatial derivatives of both the phase and the intensity distributions. For a Shack-Hartmann sensor, the phase is generally fairly smooth after reconstruction. The reconstruction process damps small amounts of noise in the data. However, this is not true for the irradiance distribution. Cross-talk between lenslets can lead to a large amount of local variation in the irradiance distribution gradient. This variation may be sensitive to the exact position of the sensor and laser beam and may change rapidly from moment to moment due to small variations of room turbulence or laser beam instabilities.

The curvature removal and multi-propagation methods, by contrast, rely on integral quantities to determine the beam parameters. These parameters are much less sensitive to small variations in beam location, threshold, or noise.

The curvature removal method relies on an accurate determination of the beam spot size. The low resolution due to the lenslet array may affect the accuracy of this calculation. Furthermore, since the camera background inherently imposes a threshold in the calculation, the spot size may be sensitive to the camera background. This threshold is not imposed on calculating the far-field spot size, and hence the two parameters needed to calculate M^2 enter into the calculation differently. This may lead to inaccuracies in the measurement.

With the multi-propagation method, all of the calculations are performed in a "gedanken" numerical space. This allows all the calculations to be performed in the same space, using the same assumptions. Furthermore, we have found that propagation from Shack-Hartmann wavefront sensor data can be accurately performed.[10] With multiple propagations, the advantages of least-squares fitting will help minimize the effect of errors or scatter.

Figure (4) shows a comparison of the gradient, curvature-removal and multi-propagation methods for a laser measured with a commercial Shack-Hartmann wavefront sensor.[11] In this case, the curvature removal and multi-propagation methods agree quite well, but the gradient method shows significant differences. It only agrees well at the measurement plane (z=0). Similar results are obtained in the y-direction. The Moments method was not included in this study. However, because of the dependence upon the numerical derivatives of the irradiance distribution, it is expected to behave similarly to the Gradient Method.

The other beam parameters that can be calculated are the location of the waist (z_0), the size of the waist (d_0), the far field divergence angle (Θ), and the Rayleigh range. Table (1) shows a comparison of these parameters for the same beam data, calculated with the different methods. The curvature Removal and Multi-Propagation methods agree well. However, the Gradient Method shows considerable error. Although the Moments method was not included in this study, the results are expected to be similar to the Gradient method because of the numerical derivatives.

In Figure (5), a sequence of the same data set was processed using the Multi-Propagation and Gradient methods for comparison. The Gradient method is significantly more sensitive to noise and other effects and produces M^2 values with 12 times higher peak-to-valley variation. In Table (2), the statistical results from the beam shown in Figure (5) are presented. The Multi-Propagation method has the least variation, followed by the Curvature Removal method. The Gradient method is clearly less accurate. However, the computation time is exactly the opposite. The fastest method is the Gradient, followed by the Curvature Removal and Multi-Propagation respectively. The Multi-Propagation takes 15–20 seconds to complete, while the Gradient Method takes less than a second. One of the difficult parameters to adjust is the camera background that is used in the calculation. For a Shack-Hartmann sensor, this becomes increasingly important because of the need to isolate the focal spots in the image prior to centroiding. There are a number of sophisticated algorithms under development that may be used for this purpose. However, the irradiance distribution is determined by integrating all of the pixel elements associated with each lenslet. To obtain an accurate measurement of the irradiance distribution, the camera background must be properly considered. This results in either camera background subtraction or thresholding at a fixed value. Some of the methods for calculating beam parameters are sensitive to the value of this setting. In Figure (6), the camera background threshold setting was varied for a 10-bit digital wavefront sensor camera (1024 total counts) with nearly saturated peak irradiance. The Gradient method is clearly sensitive to this parameter even for very small changes in the setting of this threshold. However, neither the Curvature Removal method nor the Multi-Propagation method shows significant sensitivity. It is interesting to note that the RMS wavefront error shows some sensitivity for low backgrounds. This is probably due to the fact that the wavefront becomes completely un-physical for extremely small values.

The M^2 should be completely independent of the measurement position along the beam. To test this, the wavefront sensor was placed at different locations along the beam and the beam parameters were

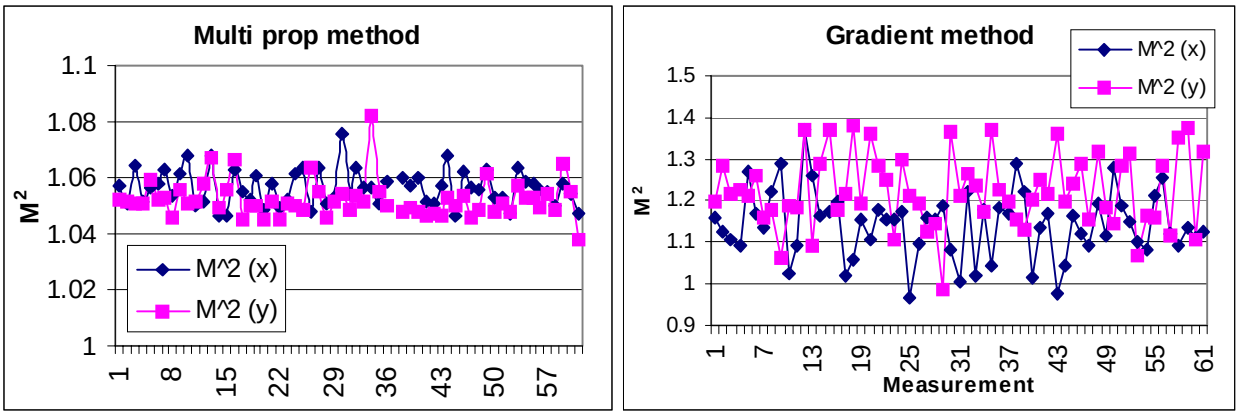

(a) (b)

Figure 5: Comparison of Multi-Propagation and Gradient methods on the same data. Measurement sequence is a series of separate measurements of the same beam.

computed from single frame measurements at each location. This resulted in the data that is presented in Figure (7). In this case, the M^2 is relatively constant for a wide range of positions. We did find that it was important to have sufficient samples across the beam in order to get accurate results. The Curvature Removal method was particularly sensitive to a lack of samples across the beam, although it was often till able to compute a reasonable M^2.

4. EVALUATION OF OPTICAL ERRORS USING BEAM QUALITY PARAMETERS

For the evaluation of optical elements that are used to transport laser beams through an optical system, it seems to be natural to use the beam quality parameters such as M2. In some cases, it may be very useful to locate the waist and determine its size. In other cases, it may be desirable to match beam parameters to other parts of the optical system. This is true in optical communications systems where fiber optics collimators are used to couple fibers to modulators and other elements. Many of these systems are close approximations of a Gaussian beam, so M^2 becomes a natural parameter to be used to evaluate system and component performance. This is valid as long as an accurate value of M^2 exists and can be measured.

Method	Mulit-Prop		Gradiant		Curvature removal	
	x	y	x	y	x	y
z_0	-0.974	-1.032	-0.680	-0.661	-0.871	-1.041
d_{s0} (mm)	0.910	0.932	1.043	1.138	0.875	0.874
M^2	1.128	1.263	1.534	1.863	1.110	1.236
Θ (mr)	0.999	1.092	1.018	1.129	1.0224	1.14
Z_R	0.911	0.853	0.879	0.862	0.856	0.766

Table1: Comparison of beam parameters using different methods.

Method	Multi-Prop		Gradient		Curvature removal	
	x	y	x	y	x	y
M^2 Ave	1.056	1.052	1.143	1.224	1.043	1.034
M^2 Std	0.006	0.007	0.081	0.089	0.022	0.016

Table 2: Statistics of 61 frame sequential analysis of the same laser beam.

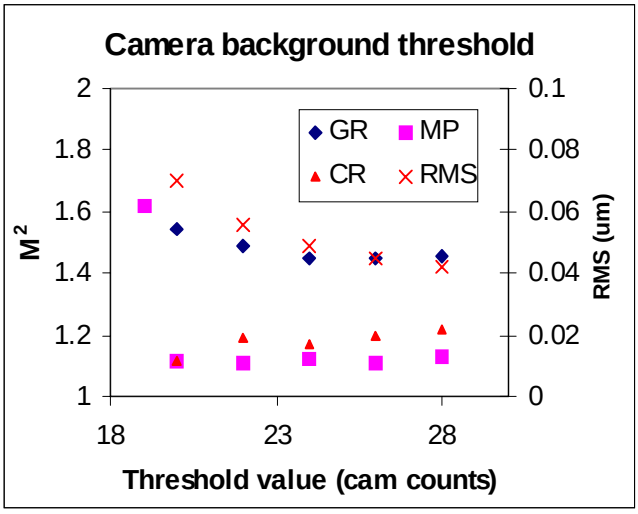

Figure 6: Effect of camera background on calculation of M2 using various methods. The RMS wavefront error is also included (X) for comparison.

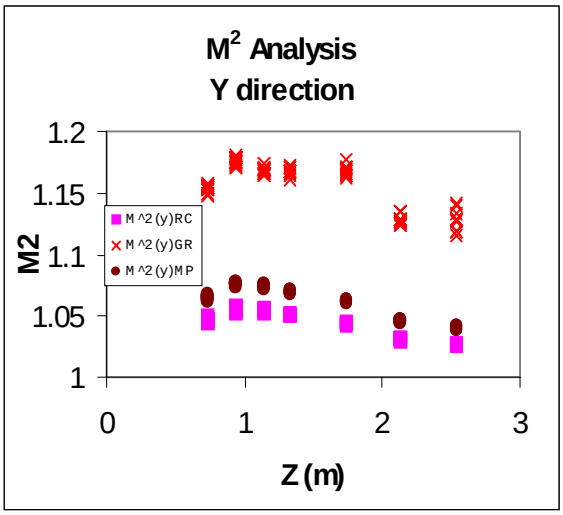

Figure 7: M2 calculated at different positions along a beam. Multiple measurements at each location can be seen as spread in the data sets. The beam waist was very near z=0.75 m, so the beam was very small at this location.

Another parameter that has long been used in evaluating the performance of optical elements is the RMS wavefront error. This can be directly measured using a wavefront sensor with a minimum of additional calculations. The purpose of this paper is to compare the RMS wavefront error parameter to the other beam quality parameters. To this end, a simple experiment was prepared as shown in Figure (9). In this experiment a HeNe laser beam was attenuated using a pair of high quality prisms and then passed through an optic under test. The beam was measured both with and without the optic, and the results were compared using the various measurements. In Figure 8, three wavefronts that are 50-frame averages of the wavefront are presented. The first is the baseline case, without a test optic in place. The other two cases are for different test optics. The optics chosen in this case were optics that are used in a commercial component. As such, they are high-quality parts, so their total wavefront error was very small. Because a highly aberrated part is easily measured with a number of methods, this was considered to be a realistic test for this work. It is only for a high quality part that differences in the various methods might be important.

In Figure (8), the total wavefront error is quite small, considering all the measurements. However, the differences are clearly distinguishable in both the distribution and the RMS values. In both test optic cases, the RMS wavefront error increased after passing through the test optic, although only a

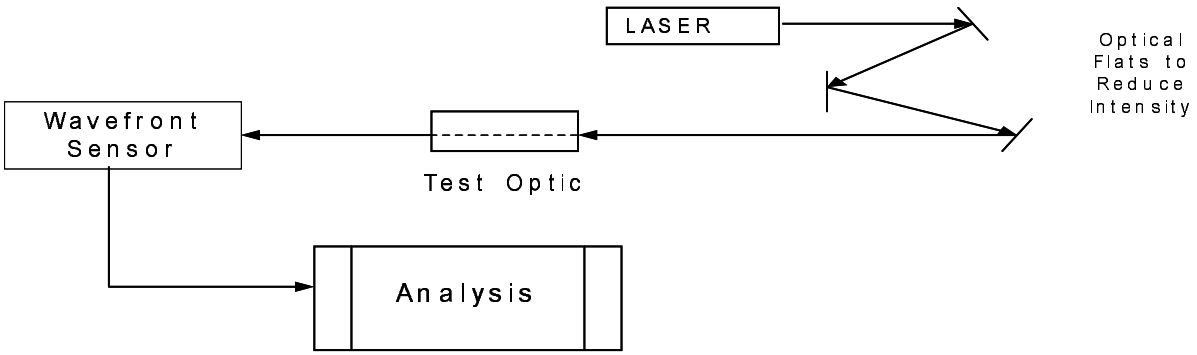

Figure 8: Experimental layout for optical testing.

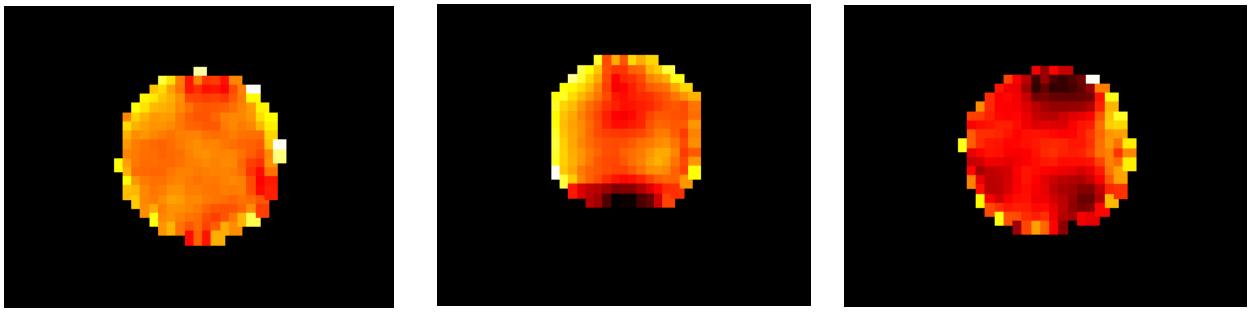

Baseline

(a) PV: 0.1322 µm

Optic 13446

(b) PV: 0.1347 µm

RMS: 0.0088 µm

Optic 13447

(c) PV: 0.1051 µm

RMS: 0.0059 µm

Figure 9: Wavefront error distributions for (a) raw laser beam, (b) Optic 13446 and (c) Optic 13447

very small amount. These very small differences were real and repeatable, but represent only a few nanometers of total RMS wavefront error. Clearly the direct wavefront measurement is an extremely sensitive measure of optical performance.

By comparison, the beam parameters were calculated from the same data (50 frame averages) that was presented in Figure (8). This data, presented in Table(3), shows three different methods. While the RMS wavefront error clearly rose when a test optic was used, an increase in M^2 was not as discernable. The increase in M^2 was masked by the accuracy of calculating the beam parameters. This limits the usefulness in this case for determining the performance of the optic.

5. CONCLUSIONS

A number of different methods were developed and compared for the estimation of the beam parameters associated with propagation of a laser beam.

The accuracy and precision of estimating these parameters depends strongly on the analysis method. This is because of numerical error propagation through the very complicated algorithms. Two new methods, the curvature removal and the multiple-propagation method, were developed and had significantly better accuracy than the previous methods (Gradient and Moments).

The RMS wavefront error can be used to evaluate component performance. However, at least for the high quality optics tested in this study, the beam parameters were unable to distinguish a difference in optical quality, where the difference was discernible in the RMS wavefront error.

Future work involves continuing to improve the beam parameters algorithms, making a comparison using the ISO 11146 method, and using a more highly aberrated optic for the testing, so that more definitive conclusions could be drawn.

	RMS Deviation (waves)		Propagation M^2		Gradient M^2		Curvature Removal M^2	
	Average	S.D.	Average	S.D.	Average	S.D.	Average	S.D.
Baseline	0.1924	2.67	1.0570	1.3245	1.1210	8.5638	1.0480	2.0992
Optic 1	0.1516	2.19	1.0450	0.6699	1.0460	8.6998	1.0310	1.6489
Optic 2	0.1557	3.42	1.0520	0.5703	1.1830	9.3829	1.0360	1.5444

Table3: Comparison of measured beam parameters and RMS wavefront error sing different M^2 methods.

ACKNOWLEDGEMENTS

The discussions and critique of K. A. Neal, K. L. Ratté and D. M. Topa are gratefully acknowledged.

REFERENCES

1. L. Marshall, *Laser Focus*, 26-28, April, 1971.
2. A. E. Siegman, *Lasers*, 696-697, University Science Books, Mill Valley, CA, 1986.
3. A. E. Siegman, "New developments in laser resonators," *SPIE Optical Resonators*, Vol. **1224**, 2-14, 1990.
4. International Standards Organization, *Lasers and laser-related equipment; Test methods for laser beam widths, divergence angle and beam propagation ratio*, **ISO/WD 11146**, 2001-03-23.
5. D. R. Neal, W. J. Alford, J. K. Gruetzner, and M.E. Warren, "Amplitude and phase beam characterization using a two dimensional wavefront sensor," *SPIE* **2870**, pp. 72-81 (1996).
6. R. Mästle, A. Giesen, and H. Hügel, "On the errors in the characterization of laser beams with wavefront sensors," 6th International Conference on Laser Beam and Optics Characterization, Munich, Bavaria, June 2001.
7. A. E. Siegman, "Defining the effective radius of curvature for a non-ideal optical beam," *IEEE J. Quant. Elec.*, **27**(5) (May 1991), pp. 1146-1148.
8. B Schafer and K. Mann, "Characterization of laser beams using a Hartmann-Shack wavefront sensor measurements," 6th International Conference on Laser Beam and Optics Characterization, Munich, Bavaria, June 2001.
9. B. J. Neubert, G. Huber, W. D. Scharfe, "On the problem of M^2 analysis using Shack-Hartmann measurements," *J. Phys.D: Appl.Phys.* **34**, (2001).
10. D. R. Neal, E. Hedlund, M. Lederer, A. Collier, c. Spring, and W. Yanta, "Shack-hartmann wavefront sensor testing of aero-optic phenomena," 20th AIAA Advanced Measurement and Ground Testing Technology Conference, *AIAA*, **98-2701**, (June 15-18, 1998).
11. *CLAS-2D*™ is a commercial Shack-Hartmann wavefront sensor provided by WaveFront Sciences, Inc., 14810 Central SE, Albuquerque, NM 87123